

Applied and Environmental Microbiology



Genetics and Molecular Biology | Full-Length Text

Fitness trade-offs of multidrug efflux pumps in *Escherichia coli* K-12 in acid or base, and with aromatic phytochemicals

Yangyang Liu,¹ Andrew M. Van Horn,¹ Minh T. N. Pham,¹ Bao Ngoc N. Dinh,¹ Rachel Chen,¹ Slaybrina D. R. Raphael,¹ Alejandro Paulino,¹ Kavya Thaker,¹ Aaryan Somadder,¹ Dominick J. Frost,¹ Chelsea C. Menke,¹ Zachary C. Slimak,¹ Joan L. Slonczewski¹

AUTHOR AFFILIATION See affiliation list on p. 16.

ABSTRACT Multidrug efflux pumps are the frontline defense mechanisms of Gram-negative bacteria, yet little is known of their relative fitness trade-offs under gut conditions such as low pH and the presence of antimicrobial food molecules. Low pH contributes to the proton-motive force (PMF) that drives most efflux pumps. We show how the PMF-dependent pumps AcrAB-ToIC, MdtEF-ToIC, and EmrAB-ToIC undergo selection at low pH and in the presence of membrane-permeant phytochemicals. Competition assays were performed by flow cytometry of co-cultured Escherichia coli K-12 strains possessing or lacking a given pump complex. All three pumps showed negative selection under conditions that deplete PMF (pH 5.5 with carbonyl cyanide 3-chlorophenylhydrazone or at pH 8.0). At pH 5.5, selection against AcrAB-ToIC was increased by aromatic acids, alcohols, and related phytochemicals such as methyl salicylate. The degree of fitness cost for AcrA was correlated with the phytochemical's lipophilicity (logP). Methyl salicylate and salicylamide selected strongly against AcrA, without genetic induction of drug resistance regulons. MdtEF-ToIC and EmrAB-ToIC each had a fitness cost at pH 5.5, but salicylate or benzoate made the fitness contribution positive. Pump fitness effects were not explained by gene expression (measured by digital PCR). Between pH 5.5 and 8.0, acrA and emrA were upregulated in the log phase, whereas mdtE expression was upregulated in the transition-to-stationary phase and at pH 5.5 in the log phase. Methyl salicylate did not affect pump gene expression. Our results suggest that lipophilic non-acidic molecules select against a major efflux pump without inducing antibiotic resistance regulons.

IMPORTANCE For drugs that are administered orally, we need to understand how ingested phytochemicals modulate drug resistance in our gut microbiome. Bacteria maintain low-level resistance by proton-motive force (PMF)-driven pumps that efflux many different antibiotics and cell waste products. These pumps play a key role in bacterial defense by conferring resistance to antimicrobial agents at first exposure while providing time for a pathogen to evolve resistance to higher levels of the antibiotic exposed. Nevertheless, efflux pumps confer energetic costs due to gene expression and pump energy expense. The bacterial PMF includes the transmembrane pH difference (ΔpH), which may be depleted by permeant acids and membrane disruptors. Understanding the fitness costs of efflux pumps may enable us to develop resistance breakers, that is, molecules that work together with antibiotics to potentiate their effect. Nonacidic aromatic molecules have the advantage that they avoid the Mar-dependent induction of regulons conferring other forms of drug resistance. We show that different pumps have distinct selection criteria, and we identified non-acidic aromatic molecules as promising candidates for drug resistance breakers.

Editor Ning-Yi Zhou, Shanghai Jiao Tong University, Shanghai, China

Address correspondence to Joan L. Slonczewski, slonczewski@kenyon.edu.

Yangyang Liu and Andrew M. Van Horn contributed equally to this article. The author order was based on seniority.

The authors declare no conflict of interest.

See the funding table on p. 16.

Received 20 November 2023 Accepted 14 December 2023 Published 30 January 2024

Copyright © 2024 American Society for Microbiology. All Rights Reserved.

February 2024 Volume 90 Issue 2

KEYWORDS AcrAB-TolC, MdtEF-TolC, EmrAB-TolC, multidrug efflux pump, phytochemicals, lipophilicity (logP), flow cytometry, relative fitness, proton-motive force, salicylate, CCCP, dPCR

The global public health threat of multidrug resistance (resistance of one strain to three or more antibiotics) (1, 2) requires us to discover new antibiotics and to find ways of reversing or breaking resistance (3, 4). Among the various mechanisms of drug resistance, bacteria encode efflux pumps that act as a frontline defense by pumping out low levels of antibiotics (5). Efflux pumps evolved as general-purpose waste transporters that export a variety of substrates, including biosynthesis intermediates (6). These pumps support the cell's fundamental metabolism and growth (7). However, these general transporters can also be overexpressed to enable low-level resistance that provides enough time for bacteria to evolve higher levels of resistance (8).

To study efflux pumps and identify resistance (3, 9), our lab investigates evolutionary trade-offs between strains that possess the pump and those that do not. We are especially interested in trade-offs associated with aromatic phytochemicals and related molecules (10–12). The fitness costs of efflux pumps might arise by various means, such as the expense of their gene expression, the cytoplasmic effects of a phytochemical, and the depletion of energy spent to export substrates. Five of the six major families of efflux pumps are powered by proton-motive force (PMF), whereas one family of pumps, the ABC transporters, is powered by ATP (6).

For our investigation of fitness trade-offs, we chose three *Escherichia coli* efflux pumps for which knockout mutations arise during long-term evolution experiments with organic acids that incur energy stress (10, 13, 14). The most studied efflux pump in Gram-negative bacteria is AcrAB-TolC, a member of the resistance-nodulation division (RND) superfamily (6, 15). AcrAB-TolC exports diverse lipophilic substrates such as β-lactam, quinolone, and macrolide antibiotics, as well as bile acids, polyphenols, and organic solvents (7, 16–19). Another PMF-dependent RND pump is MdtEF-TolC (20, 21). MdtEF-TolC exports many of the same substrates as AcrAB-TolC (22), but it is preferentially expressed under the stationary phase and at low pH, and it is essential for extreme acid survival (19, 22, 23). The EmrAB-TolC MDR pump belongs to the major facilitator superfamily, though its tripartite structure resembles that of RND pumps (24). EmrAB-TolC exports PMF uncouplers such as dinitrophenol, carbonyl cyanide 3-chlorophenylhydrazone (CCCP), and carbonyl cyanide 4-(trifluoromethoxy)phenylhydrazone (FCCP) (25) as well as colistin, quinolone, and bile acids (19, 26, 27).

We investigate the basis of energy-stress trade-offs related to pH and PMF. *E. coli* adapts to growth at a range of external pH 5.0–9.0 (28, 29), which is typically found in the human intestinal tract (30, 31). Low external pH increases the transmembrane pH difference (Δ pH) component of the PMF available to run efflux pumps (32). The increased Δ pH (and therefore PMF) can increase the rate of drug efflux (33). At the same time, efflux pumps may compete with other PMF-intensive cell functions. For example, the deletion of AcrAB-TolC increases flagellar motility, which varies with proton-motive force (34, 35). Low pH also amplifies the uptake of membrane-permeant weak acids that can impair cell growth in various ways and can reverse antibiotic resistance (10).

Antibiotic resistance can be reversed by various phytochemicals (36) and microbial natural products, particularly aromatic molecules (36, 37). Aromatic carboxylates decrease the pump fitness contribution (11). Alternatively, cell function may be impaired by proton leak, as studied in mitochondria (38–40). Protons leak through ATP synthase and other membrane proteins (41).

Certain lipophilic molecules induce membrane leaks that deplete PMF (42). A measure of lipophilicity is logP, the octanol-water partition coefficient, which is commonly considered in the assessment of pharmaceutical candidates (43). More lipophilic molecules with higher logP will tend to associate with the inner membrane. Lipophilic molecules might also affect efflux pumps by destabilizing the membrane-embedded substrate-binding pockets of pump substrates such as AcrB (44, 45).

Finally, if an upregulated drug pump is not important for survival under a given condition, such as low pH or the presence of an inhibitory phytochemical, the corresponding drug pump genes would confer a negative fitness cost to the cell and be selected against. Thus, the selective effects that phytochemicals and aromatic molecules have on drug pumps may also result from their effects on the expression of drug pump genes.

Here, we used relative fitness assays by flow cytometry co-culture to explore the fitness trade-offs of AcrAB-ToIC, MdtEF-ToIC, and EmrAB-ToIC in the presence of a variety of naturally occurring organic molecules with diverse chemical properties (46, 47). We aimed to distinguish the basis of their effects with respect to pH stress, PMF stress, lipophilicity (membrane solubility), and gene expression. Our findings suggest promising ways to develop resistance breakers that potentiate antibiotics by decreasing the frontline drug resistance of pathogens.

RESULTS

Competition assays by co-culture with flow cytometry

The relative fitness contributions of MDR efflux pumps were measured by flow cytometry in short-term weekly competition experiments (11, 12) as described under Materials and Methods. In these experiments, a strain that carries a pump gene defect, such as ΔacrA::kanR, is co-cultured with the parent strain W3110 ΔyhdN::kanR (acrA+) for approximately 30 generations over 3 days (Fig. 1). Each strain expresses a different fluorophore, yellow fluorescent protein (YFP) or cyan fluorescent protein (CFP), which identifies cells by flow cytometry (see Table 1 for strains). The slope of YFP/CFP log₂ ratios provides a measure of relative fitness for the pump deletion strain. To minimize the risk of fluorophore-specific selection effects, for each experimental condition, an equal number of trials use the YFP label for the deletion strain and for the parent strain, respectively.

During passage through the digestive tract, enteric bacteria experience a wide range of pH conditions, from the stomach (pH 1.0-4.0) to the small intestine (pH 5.0-6.5) and the colon (pH 5.0-8.0) (30, 49). We compared the relative fitness contributions of efflux pumps during culture at pH values representative of the intestinal range (pH 5.5 and 8.0). We then tested the effects of various phytochemicals and related small molecules added to the culture media at pH 5.5. For all trials, statistical tests are presented in Table S1.

PMF depletion by CCCP or at high external pH decreases the relative fitness of efflux pumps

We tested the PMF dependence of efflux-pump fitness contributions by measuring relative fitness of pump deletion strains under several conditions that lead to different levels of PMF (Fig. 2A). Each pump deletion (ΔacrA::kanR, ΔmdtE::kanR, and ΔemrA::kanR) was tested at pH 5.5, a condition under which ΔpH is large, and the overall PMF (comprising ΔpH and $\Delta \psi$) is maximized. The relative fitness of each pump was also tested at pH6.8, a condition under which ΔpH (and thus PMF) is somewhat lower. Compared to pH 5.5, at pH 6.8 the AcrA and EmrA pumps decreased fitness, whereas the MdtE pump showed no significant difference.

The pump fitness contributions were also tested under conditions where PMF is low: growth at external pH 8.0, where the ΔpH is inverted and leaves a small electrical potential ($\Delta \psi$) as the sole source of PMF; and growth with 10 μ M CCCP at external pH 5.5, where the PMF is drained by the uncoupler. At pH 8.0, where the overall PMF is low, all three pumps decreased the relative fitness (Fig. 2A). In each competition, the parental strain each produced about half as many progenies per day as the respective deletion strain ($\Delta acrA$, $\Delta mdtE$, and $\Delta emrA$, respectively). All three pump genes showed similar fitness disparities of about one log₂ unit between growth at pH 5.5 and pH 8.0.

The $\triangle acrA$ and $\triangle mdtE$ strains showed comparable growth disparities in CCCP at pH 5.5 (Fig. 2A). Thus, AcrAB-TolC and MdtEF-TolC each conferred a fitness cost compared to a

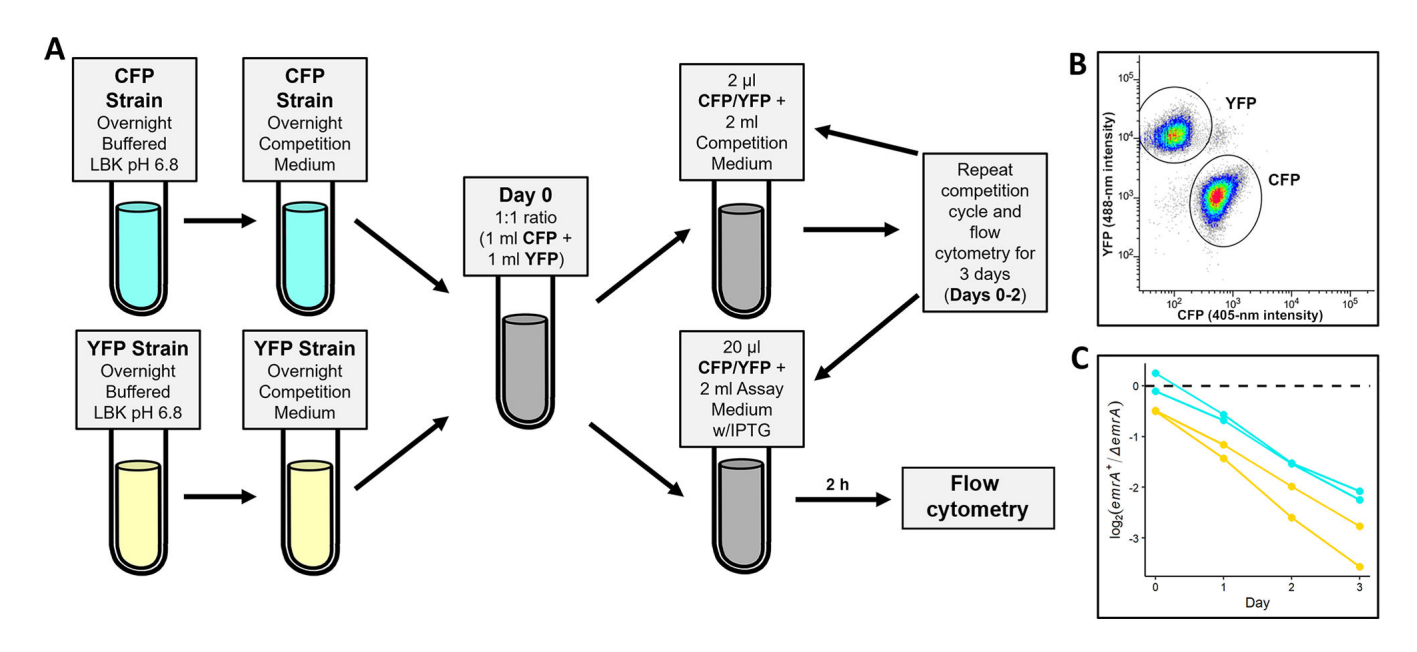


FIG 1 Relative fitness competition assay using flow cytometry (11). (A) Daily cell co-culture was diluted 100-fold and incubated with isopropyl β-D-1 thiogalactopyranoside (IPTG) for 2 h to induce fluorescent protein expression. (B) Fluorescence intensity distribution of co-cultured YFP and CFP populations is identified by flow cytometry. The YFP-expressing population shows high-intensity emission from the 488 nm laser (Y axis) and low-intensity emission from the 405 nm laser (X axis), whereas the CFP-expression population shows the reverse pattern of emission. (C) Example of a line plot displays log₂ ratios of the pump-expressing population divided by the pump-deleted strain (emrA*/\(Delta mrA\)). The log2 population ratios are compiled for Day 0 through Day 3 for a total of ~30 generations. The slope of the log₂ population ratios over time [doublings per day gives the selection ratio (a measure of relative fitness) for the pump, in this case, EmrAB-ToIC]. For each experimental condition, an equal number of trials were performed with the pump deletion linked to YFP or CFP. For all figures, statistical tests are presented in Table S1.

strain deleted for a pump gene ($\Delta acrA$ or $\Delta mdtE$, respectively). The selection for EmrAB-TolC, however, showed a wide variance with an overall positive selection for the pump. Since CCCP is a substrate of EmrAB-ToIC (25), the pump may provide a fitness advantage that partly compensates for PMF depletion.

To confirm that CCCP decreases PMF, we measured cytoplasmic pH in cells treated with 10 µM CCCP (Fig. 2B). The periplasmic pH of E. coli is equal to that of extracellular pH (50) and, therefore, allows us to determine the Δ pH across the inner membrane. The electrical potential also contributes to PMF but is not practical to measure in E. coli under our conditions (51, 52). The cytoplasmic pH was measured by use of a strain expressing the ratiometric protein fluorophore pHluorin [(28) described under Materials and Methods]. A small but significant decrease in cell pH depression was observed with 10 μM CCCP (approximately -0.2 units). A much larger pH decrease was shown in the presence of 100 µM CCCP (about -2.0 units), a concentration that prevents growth.

TABLE 1 E. coli strains used in this study

Strain	Genotype	Source
W3110	E. coli K-12 F λ	Lab stock (48)
JLS1105	W3110 pGFPR01(PBAD pHluorin bla)	Lab stock (28)
JLS1910	W3110 ΔgalK::PLlacO-1 cfp-bla, ΔyhdN::kanR	Lab stocks (11)
JLS1911	W3110 ΔgalK::PLlacO-1 yfp-bla, ΔyhdN::kanR	
JLS1826	W3110 ΔgalK::PLlacO-1 cfp-bla, ΔacrA::kanR	
JLS1832	W3110 ΔgalK::PLlacO-1 yfp-bla, ΔacrA::kanR	
JLS1834	W3110 ΔgalK::PLlacO-1 cfp-bla, ΔmdtE::kanR	
JLS1835	W3110 ΔgalK::PLlacO-1 yfp-bla, ΔmdtE::kanR	
JLS1912	W3110 ΔgalK::PLlacO-1 cfp-bla, ΔemrA::kanR	
JLS1913	W3110 ΔgalK::PLlacO-1 yfp-bla, ΔemrA::kanR	

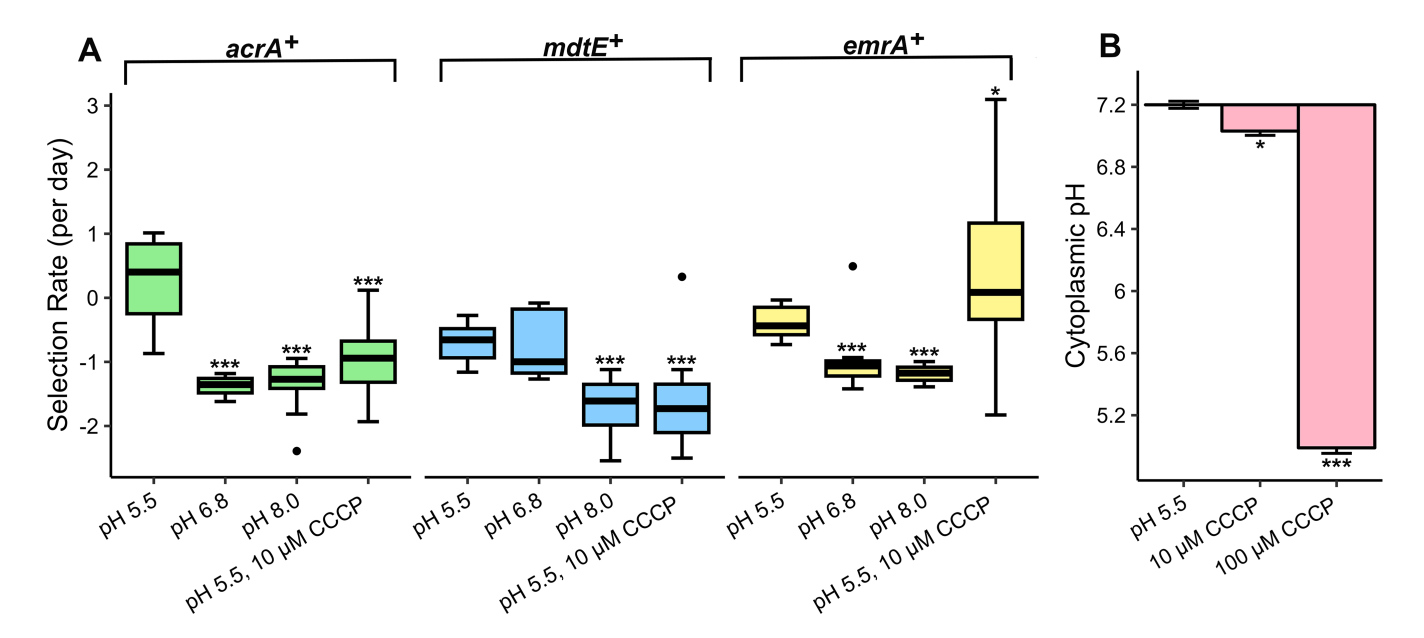


FIG 2 PMF depletion by CCCP or at high pH affects the relative fitness contributions of $acrA^+$, $mdtE^+$, and $emrA^+$. (A) Selection rate was calculated as shown in Fig. 1. Asterisks indicate the results of Mann-Whitney U tests for comparison of each 10 μ M CCCP treatment group to the corresponding pH 5.5 control for each gene tested (*P < 0.05; **P < 0.01; and ***P < 0.001). $n \ge 12$ for all conditions tested. (B) Change in cell pH indicates the mean difference in cytoplasmic pH of strain JLS1150 cells using pHluorin flow cytometry. Cells were cultured at external pH 5.5 with or without CCCP exposure for 5 min. Bars represent standard error. $n \ge 6$ for all conditions tested. Asterisks indicate results of Welch's t-tests for comparison of each CCCP treatment group to the pH 5.5 control (*P < 0.05; **P < 0.01; and ***P < 0.001). Statistical tests are presented in Table S1.

Overall, our results showed that partial depletion of PMF, either by growth at pH 5.5 with low concentration CCCP or by growth at pH 8.0, caused selection against the efflux pumps.

Weak acids depress cytoplasmic pH

Membrane-permeant weak acids can depress cell pH and decrease PMF, though requiring higher concentrations than CCCP (53, 54). In addition, the growth-inhibitory anion may accumulate in the cell in proportion to the Δ pH. Both pH depression and anion accumulation may affect the fitness contribution of efflux pumps.

We compared the depression of cytoplasmic pH by various carboxylic acids and related molecules at 1 mM concentration (Fig. 3). The dissociation constants (p K_a) of these molecules are in Table 2. The strongest pH depression was caused by salicylic acid (salicylate) (-0.8 pH units). At 1 mM concentration, benzoic acid, sorbic acid, and butyric acid all depressed cell pH by significant amounts. However, ferulic acid showed a slight increase in cytoplasmic pH (+0.2 units). A larger concentration of ferulic acid (10 mM) did depress cell pH (data not shown). The non-acidic molecules salicyl alcohol, vanillin, and salicylamide also caused slight increases in cytoplasmic pH, while benzyl alcohol and methyl salicylate showed no effect.

Lipophilic molecules select against acrA+

To investigate the mechanism of phytochemical effects on pump fitness contributions, we selected aromatic carboxylates and related small organic molecules with a range of acidity and lipophilicity (Table 2). For flow cytometry, strains with or without a given efflux pump were co-cultured at pH 5.5 in the presence of each selected molecule at 1 mM (Fig. 4). This concentration was chosen based on minimum inhibitory concentration (MIC) assays showing that 1 mM concentration of each molecule allowed growth to at least $OD_{600} = 0.7$.

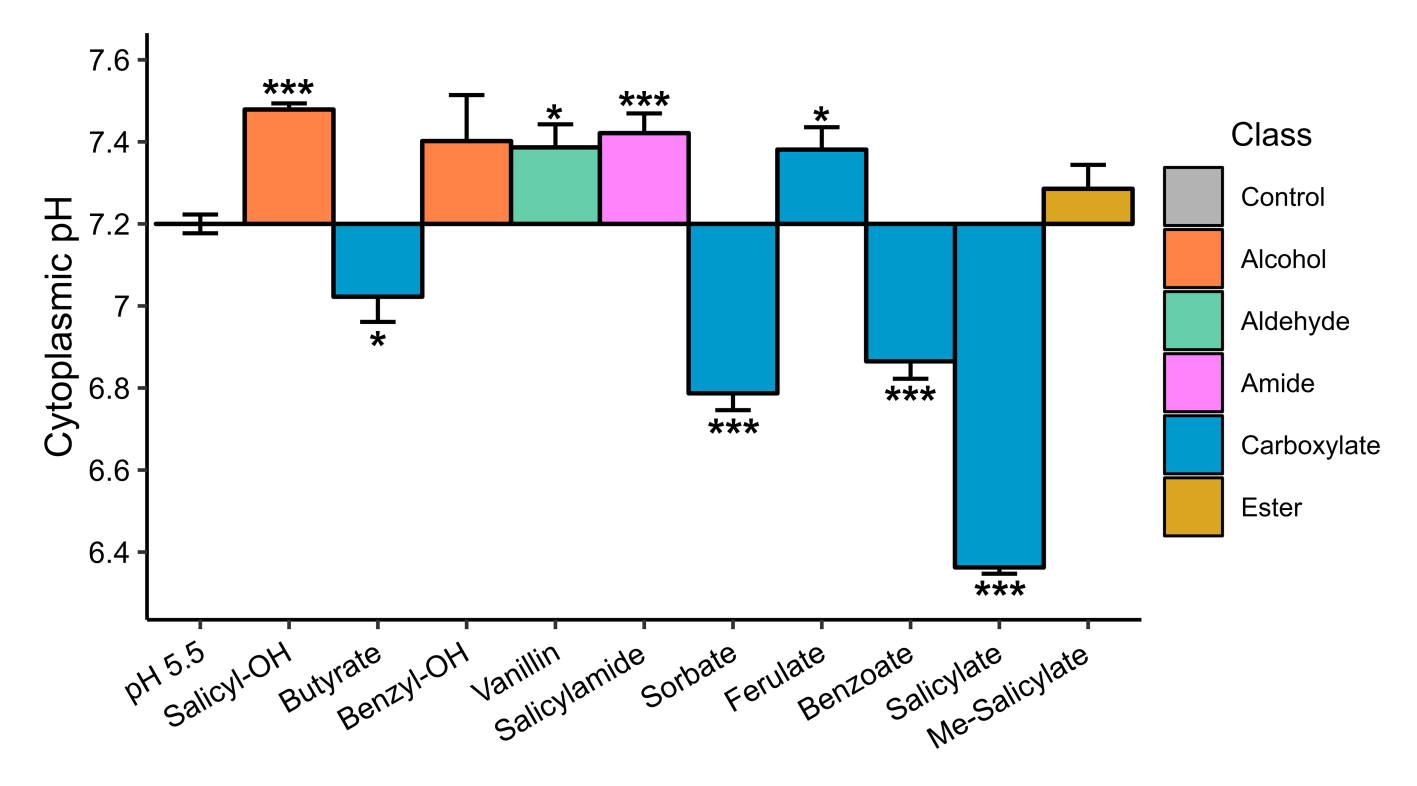


FIG 3 *E. coli* cytoplasmic pH during exposure to various organic molecules at 1 mM. Cytoplasmic pH indicates the mean pH value after exposure to a small molecule. Values of cytoplasmic pH were determined by pHluorin fluorescence using a standard curve as described under Materials and Methods. Each culture was exposed to 1 mM of the molecule for 5 min in the culture medium at pH 5.5. Colors indicate key functional groups. Bars represent the standard error of the mean. Asterisks indicate results of Welch's *t*-test for the comparison of an individual molecule to the pH 5.5 control (*P < 0.05; **P < 0.01; and ***P < 0.001). $P \ge 0.001$ for each of the molecules tested. Statistical tests are presented in Table S1.

In the pH 5.5 control, the $acrA^+$ strain ($\Delta yhdN::kanR$) had a small positive selection rate (Fig. 4A). For further experiments, the relative fitness values for all molecules tested were normalized to the median selection rate for the pH 5.5 control. Most of the molecules tested, except for butyrate, salicyl alcohol, and vanillin, selected against $acrA^+$. Salicylate showed especially strong selection against $acrA^+$ at a magnitude comparable to that found with CCCP or at pH 8.0 (Fig. 2A). But the salicylate ester, methyl salicylate, showed an equivalent size of negative selection. Thus, acidity was not essential for selection against $acrA^+$.

TABLE 2 Properties of all molecules tested in FACS competition^a

February 2024 Volume 90 Issue 2

Compound	pK _a	logP	MIC (mM)
Salicyl alcohol	9.92	0.73	>10
Butyrate	4.82	0.79	32
Benzyl alcohol	15.40	1.10	>10
Vanillin	7.91	1.26	16
Salicylamide	8.37	1.28	16
Sorbate	4.80	1.33	4
Ferulate	4.42	1.51	16
Benzoate	4.20	1.87	4
Salicylate	3.00	2.24	2
Methyl salicylate	9.80	2.55	>1
CCCP	5.95	3.38	0.032

 c pK $_a$ and logP values are sourced from the open-source PubChem database. MIC values are from assays performed twice on each strain at pH 5.5. All MIC values listed as greater than a given concentration have permitted growth at the stated concentration.

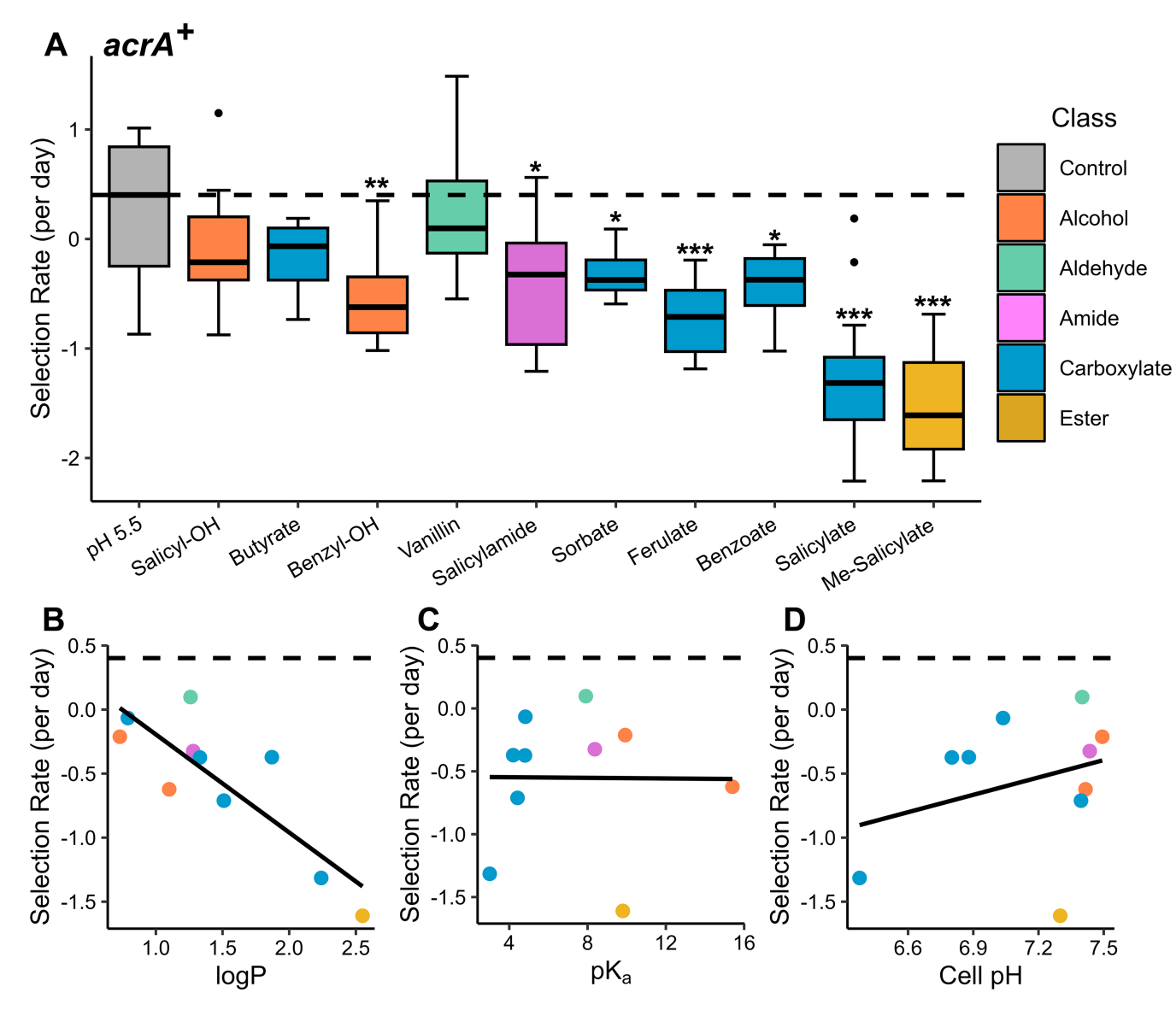


FIG 4 Selection for $acrA^{\dagger}$ pH 5.5. Selection rate was calculated as $\log_2(\Delta yhdN:kanR/\Delta acrA:kanR)/day$. Dashed line indicates the pH 5.5 control median used as a baseline for comparison. Colors indicate molecular functional groups. (A) Box plots of selection rates for $acrA^{\dagger}$. Each molecule was tested at 1 mM. Molecules are organized from left to right in increasing order by logP. Asterisks indicate results of Mann-Whitney U tests for comparison of an individual molecule to the pH 5.5 control (*P < 0.05; **P < 0.01; and ***P < 0.001). (B–D) Scatter plots of median selection rates for $acrA^{\dagger}$ in the presence of the molecules shown in the box plots with Pearson least squares line. Scatter plots show relationships between the selection rate for $acrA^{\dagger}$ and (B) $\log P$ (P = 0.708), (C) pK_a (P = 7.31 × 10⁻⁵), and (D) pH change from cell pH assays after 5 min of 1 mM exposure to the specified molecule (P = 0.095). (A–D) P ≥ 12 for all molecules tested. Statistical tests are presented in Table S1.

An important factor in molecular interactions with the bacterial envelope is lipophilicity, especially for AcrAB-ToIC, where the substrate binding pocket is immersed in the cell membrane (44, 45). A measure of lipophilicity commonly used to assess pharmaceutical agents is logP, representing the \log_{10} of the octanol-water partition coefficient (the ratio between concentrations of the molecule in octanol versus water) (43). A strong negative correlation was observed between the $acrA^+$ selection rate and the molecule's lipophilicity indicated by logP ($r^2 = 0.708$) (Fig. 4B). However, no correlation was observed between $acrA^+$ selection and pK_a ($r^2 = 7.31 \times 10^{-5}$) (Fig. 4C) nor with cytoplasmic pH depression ($r^2 = 0.095$) (Fig. 4D). Thus, for AcrAB-ToIC, the fitness trade-off incurred by aromatic carboxylates and related molecules appeared to derive from membrane solubility rather than acidity.

Salicylate and benzoate increase the fitness contributions of mdtE+ and emrA+

We examined the same set of structures (Table 2) for relative fitness assays of MdtEF-TolC. In the pH 5.5 control, mdtE+ had a negative selection rate (Fig. 5A). This finding suggests that MdtEF-ToIC decreases bacterial fitness at pH 5.5, under our culture conditions. Compared to $acrA^+$ (Fig. 2A), $mdtE^+$ incurs about one log_2 unit loss of relative fitness.

Of all the molecules tested, only benzoate and salicylate significantly affected the selection rate for mdtE+. Each of these aromatic carboxylates partly reversed the negative fitness contribution of mdtE+ at pH 5.5. Sorbate and butyrate each led to a median selection rate above that of the pH 5.5 control, although the wide variance eliminated significance.

The mdtE selection rate showed a negative correlation with the molecule's pK_a ($r^2 =$ 0.335) (Fig. 5C). Moreover, a strong negative correlation is observed ($r^2 = 0.691$) between the selection rate and the cytoplasmic pH (Fig. 3 and 5D). These results suggest that

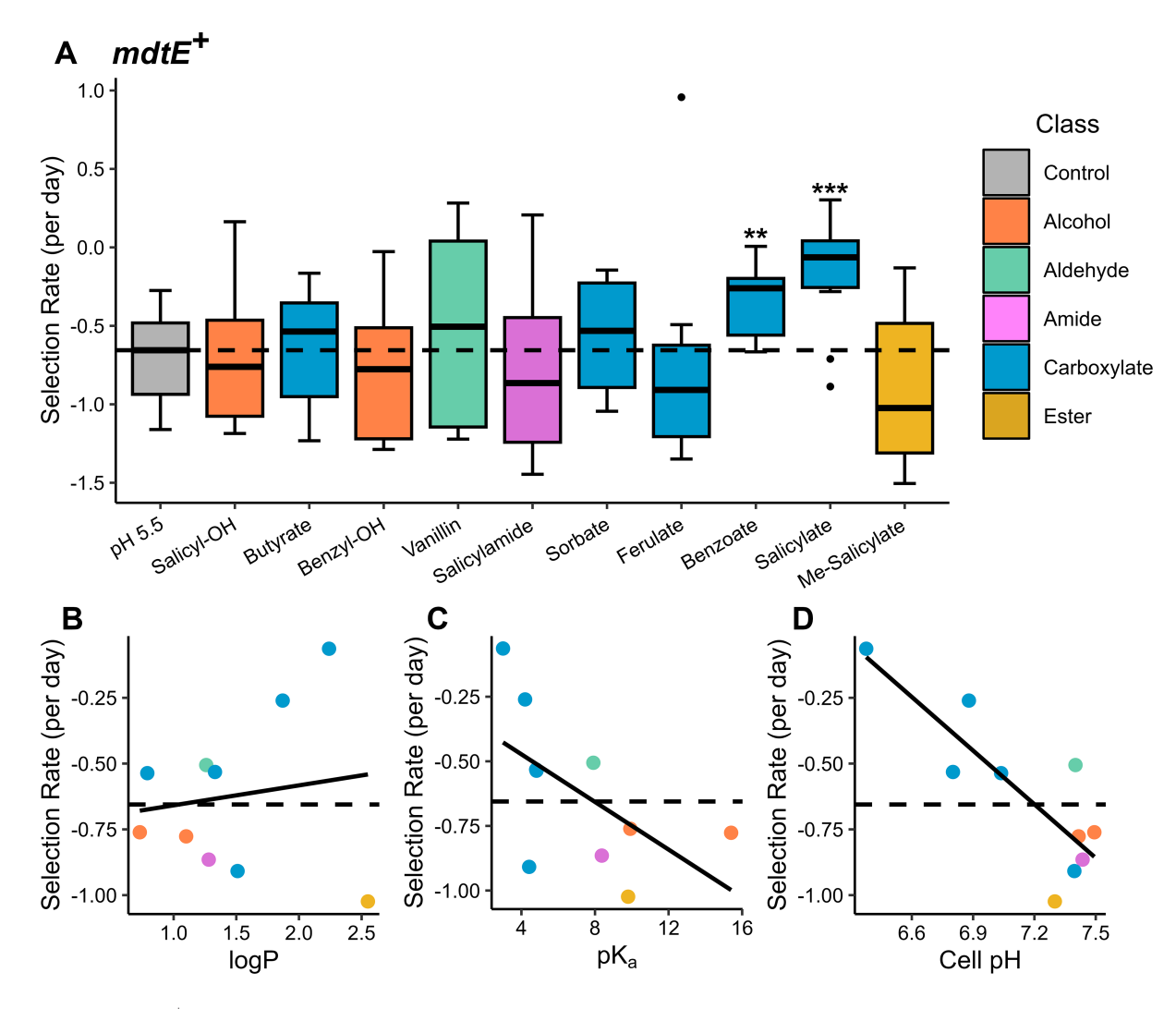


FIG 5 Selection for mdtE⁺at pH 5.5. Selection rate was calculated as log₂ (\(\Delta\)yhdN::kanR/\(\Delta\)mdtE::kanR)/day. Dashed line indicates the pH 5.5 control median used as a baseline for comparison. Colors indicate molecular functional groups. (A) Box plots of selection rates for mdtE⁺. Each molecule was tested at 1 mM. Molecules are organized from left to right in increasing order by logP. Asterisks indicate results of Mann-Whitney U tests for comparison of an individual molecule to the pH 5.5 control (*P < 0.05; **P < 0.01; and ***P < 0.001). (B-D) Scatter plots of median selection rates for mdtE⁺ in the presence of the molecules shown in the box plots with Pearson least squares line. Scatter plots show relationships between selection rate for mdt^{\pm} and (B) logP ($t^2 = 0.022$), (C) pK_a ($t^2 = 0.335$), and (D) pH change from cell pH assays after 5 min of 1 mM exposure to the specified molecule ($r^2 = 0.691$). (A–D) $n \ge 12$ for all molecules tested. Statistical tests are presented in Table S1.

molecules that decrease the cytoplasmic pH select for MdtEF-TolC. Unlike acrA+, no correlation was observed for $mdtE^+$ selection with logP ($r^2 = 0.022$) (Fig. 5B).

Similar to mdtE⁺, emrA⁺ had a negative selection rate at pH 5.5 (Fig. 6A), whereas benzoate and salicylate increased the pump's fitness contribution. Salicylamide selected against emrA+. Overall, like mdtE+, the emrA+ selection rate showed a moderate negative correlation between relative fitness and molecule p K_a ($r^2 = 0.236$) (Fig. 6C) and a strong negative correlation with the cytoplasmic pH ($r^2 = 0.736$) (Fig. 6D). Only a small correlation was observed for the emrA⁺ selection rate with logP ($r^2 = 0.127$) (Fig. 6B). Overall, both MdtEF-ToIC and EmrAB-ToIC showed a positive fitness contribution in the presence of the membrane-permeant aromatic acids salicylate and benzoate.

Expression profiles of pump genes vary with growth phase and pH

The fitness trade-offs for efflux pumps may depend on the energy costs of gene expression, which varies across the phases of growth (55). The growth phase is relevant because, in our co-culture experiments, the daily cycle of serial dilutions runs through the lag phase, log phase, and stationary phase.

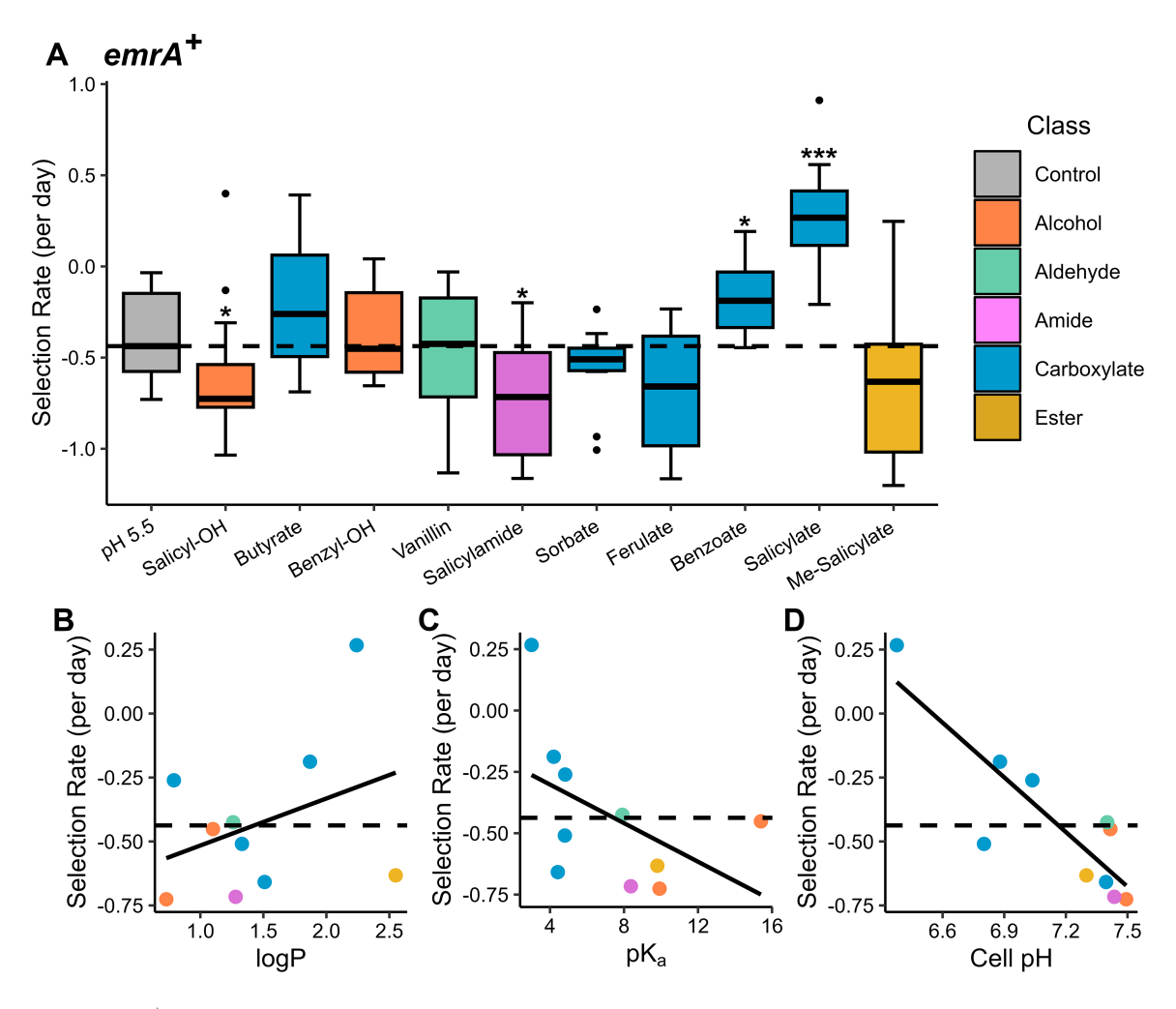


FIG 6 Selection for emrA⁺ at pH 5.5. Selection rate was calculated as log₂ (\(\Delta \text{yhdN::kanR} \seta \text{demrA::kanR} \) / day. Dashed line indicates the pH 5.5 control median used as a baseline for comparison. Colors indicate functional groups. (A) Box plots of selection rates for emrA*. All molecules were tested at 1 mM. Molecules are organized from left to right in increasing order by logP. Asterisks indicate results of Mann-Whitney U tests for comparison of an individual molecule to the pH 5.5 control (*P < 0.05; **P < 0.01; and ***P < 0.001). (B–D) Scatter plots of median selection rates for $emrA^+$ in the presence of the molecules shown in the box plots with Pearson least squares line. Scatter plots show relationships between the selection rate for $emrA^{+}$ and (B) logP ($r^{2} = 0.127$), (C) pK_{a} ($r^{2} = 0.236$), and (D) pH change from cell pH assays after 5 min of 1 mM exposure to the specified molecule ($r^2 = 0.736$). (A–D) $n \ge 12$ for all molecules tested. Statistical tests are presented in Table S1.

We quantified the expression of genes representing each of the three efflux pumps (acrA, mdtE, and emrA) by isolating RNA transcripts from cultures at three pH levels (Fig. 7). The cultures were each harvested during log phase (OD₆₀₀ = 0.1–0.2) and during the transition-to-stationary phase (OD₆₀₀ = 0.4–0.7). The OD₆₀₀ values and time of harvest of individual replicates are presented in Table S2. Transcript levels were measured using digital polymerase chain reaction (dPCR) multiplex assays (see Materials and Methods). The Taqman probe sets and fluors are presented in Table S3. Statistical tests are presented in Table S1.

The *acrA* and *emrA* genes showed higher expression in the log phase than in the transition phase. Across moderate pH levels (5.5–8.0), *emrA* expression levels were approximately half those of *acrA* expression. The *acrA* expression did not show pH dependence, but in the log phase, *emrA* showed higher expression at pH 5.5 than at pH 8.0. By contrast, *mdtE* showed higher expression in the transition phase than in the log phase, consistent with the literature (55). In the log phase, *mdtE* was upregulated strongly at pH 5.5, consistent with its inclusion in the Gad acid fitness island (56) and its evidence for acid-adapted substrate binding (22). Thus, the two pumps that showed a positive fitness contribution in the presence of salicylate or benzoate (MdtEF-TolC and EmrAB-TolC) also showed upregulation in the log phase at low external pH.

We also tested the expression effects of selected carboxylates and methyl salicylate during growth at pH 5.5 (Fig. 7). Methyl salicylate increased the log-phase expression of *acrA* but had marginal effects on *mdtE* and *emrA*. The inclusion of sorbate, benzoate, or salicylate slowed the culture growth (Table S2) and in some cases, narrowed the difference in expression between the log and transition phases. In general, no pattern of gene expression could explain the selection effects reported in Fig. 4 to 6, especially the large negative fitness contributions of salicylate and methyl salicylate for *acrA*⁺ (Fig. 4).

Non-acidic salicylate derivatives do not induce chloramphenicol and tetracycline resistance

A challenge for the development of resistance breakers has been that effective candidates such as salicylate can induce antibiotic resistance (10, 13, 57). Salicylate and related aromatic acids, such as benzoate, induce the multidrug resistance regulon Mar (58) and increase resistance to antibiotics such as chloramphenicol and tetracycline.

Since our competition assays identified lipophilic non-acids as a class of molecules that select against a major efflux pump, it is of interest to know whether these molecules induce drug resistance via Mar or other genetic systems. For two salicylate derivatives, methyl salicylate and salicylamide, we tested their effects on *E. coli* sensitivity to the clinically relevant antibiotics chloramphenicol and tetracycline. *E. coli* W3110 showed MIC values of 4 and 2 μ g/mL for chloramphenicol and tetracycline, respectively (Table 3). Consistent with previous work (13, 57), 1 mM salicylate increased the MIC of chloramphenicol and tetracycline twofold, to 8 and 4 μ g/mL, respectively. However, neither methyl salicylate nor salicylamide affected the MIC for chloramphenicol or tetracycline. The presence of methyl salicylate or salicylamide decreased the MIC for kanamycin, streptomycin, and polymyxin B. Thus, lipophilic non-acids may be a clinically promising class of resistance breakers that avoid inducing drug resistance regulons.

TABLE 3 Antibiotic MIC values in the presence of salicylate derivatives^a

Antibiotic (μg/mL)	Molecule added (1 mM)		dded (1 mM)	
	None	Methyl salicylate	Salicylamide	Salicylate
Chloramphenicol	4	4	4	8
Kanamycin	32	16	16	8
Polymyxin B	4	2	2	2
Streptomycin	32	16	16	8
Tetracycline	2	2	2	4

 $^{\circ}$ MIC values (µg/mL) for *E. coli* W3110 cultured at pH 6.8 with 1 mM of various salicylate derivatives and various antibiotics. MIC values listed are the lowest concentration of antibiotics that prevented growth to OD₆₀₀ > 0.05 after 22 h. Results shown are representative of nine trials across three separate experiments.

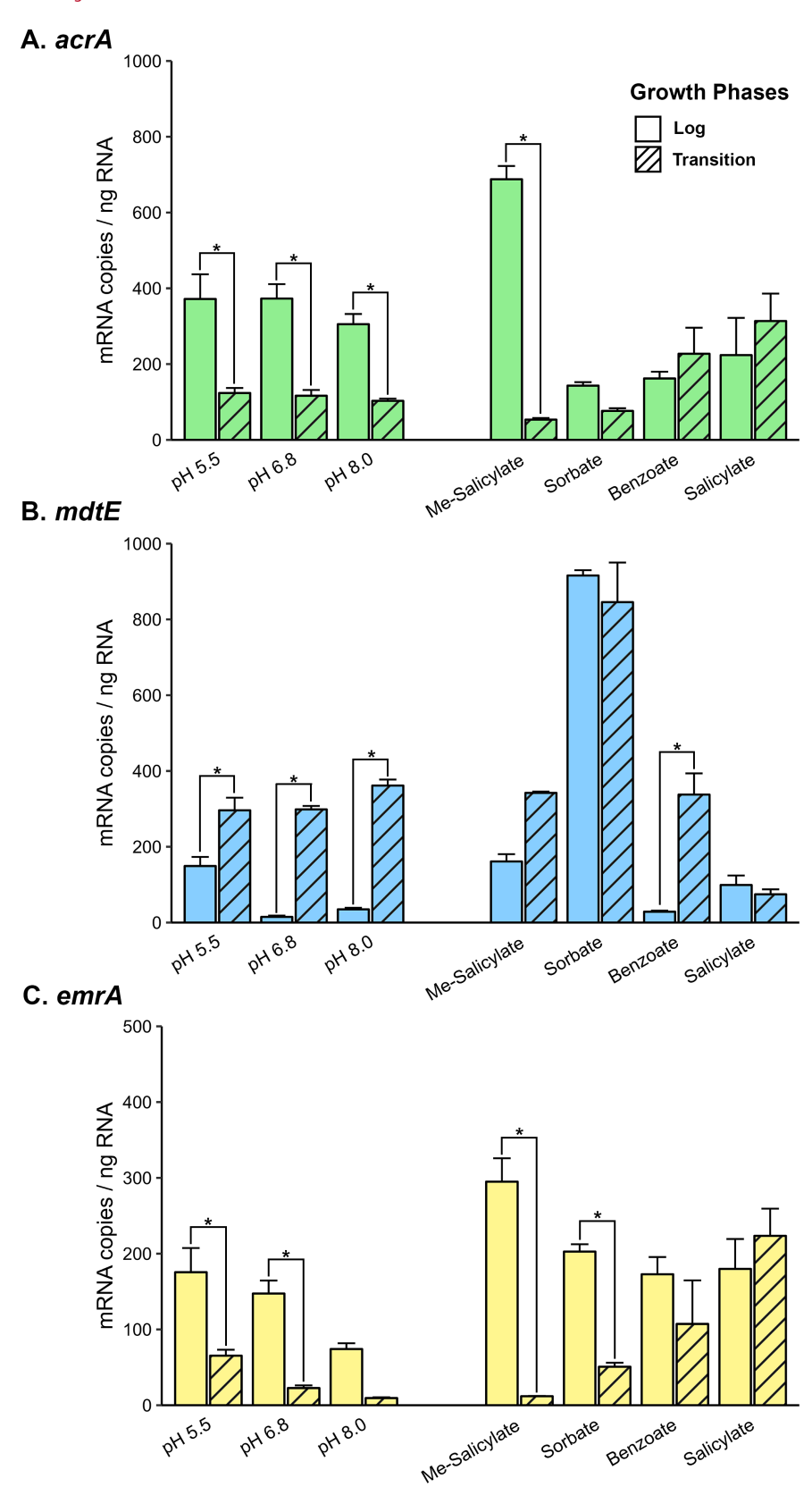


FIG 7 Gene expression for *acrA*⁺, *mdtE*⁺, and *emrA*⁺ under various conditions of pH and added molecules. *E. coli* K-12 W3110 was cultured to the log phase and transition-to-stationary phase in LBK buffered at pH 5.5, pH 6.8, and pH 8.0 (Table S2). Gene expression was measured by multiplex dPCR. The dPCR probe sets (Continued on next page)

FIG 7 (Continued)

used were for (A) acrA, (B) mdtE, and (C) emrA (Table S3). For each probe set, the mRNA expression levels were normalized by dividing the transcript concentrations measured in dPCR (copies/ μ L) by the total RNA concentrations (ng/μ L) of the samples used. Colors represent MDR pump genes and bar patterns represent growth phases. Error bars represent 1 SEM. Numbers along the x-axis correspond to the median pH. Each added molecule was tested at 1 mM. Two-way ANOVA and $post\ hoc$ least squares difference with the Benjamini-Hochberg correction were used to compare expression levels of individual efflux pump genes across all tested conditions. Statistical tests are presented in Table S1.

DISCUSSION

Efflux pumps serve bacteria with multiple functions for waste excretion and defense. In natural microbiomes, including those of the digestive tract, the drug resistance mediated by efflux pumps might be decreased by the presence of naturally occurring phytochemicals that act as resistance breakers (3, 4, 9). However, the basis of phytochemical resistance breakers is poorly understood.

Our study explored three distinct levels at which phytochemicals could impact selection: the energetic level, the expression level, and the substrate level. First, we demonstrated that an inverted ΔpH could select against all three efflux pumps. However, we also showed that molecules that depress cytoplasmic pH selected for both $mdtE^+$ and $emrA^+$ but showed no relationship with $acrA^+$ selection. This suggests that ΔpH depletion by phytochemicals alone was not sufficient to select against efflux pumps. We also characterized the fitness effects of efflux pump gene expression but found no expression differences that explained selection rates. Therefore, our data suggest that efflux pump selection is regulated primarily at the level of pump physiology. This suggests that efflux pump physiology and function must be considered in the development of effective resistance breakers.

We found some common physical-chemical principles associated with molecules that select against *E. coli* strains with multidrug efflux pumps. Partial depletion of PMF, by growth with CCCP or at high pH, incurs strong selection against all three efflux pumps tested (Fig. 2). This negative selection makes sense given the load on PMF incurred by these pumps.

Other fitness effects differed among the three pumps tested. Neither PMF nor cytoplasmic pH depression explains the *acrA*⁺ selection rates observed in the presence of various phytochemicals including non-acidic molecules such as methyl salicylate and salicylamide (Fig. 4). However, the *acrA*⁺ selection rates in the presence of the molecules tested were highly correlated with the lipophilicities of these compounds (Fig. 4B). Lipophilicity determines a molecule's ability to integrate into the bacterial inner membrane, where it can interact with the membrane-embedded substrate-binding domain of AcrB in the AcrAB-TolC pump (44, 45). Such a mechanism might explain the selective effects of lipophilic non-acids such as methyl salicylate (59, 60). AcrAB-TolC effluxes primarily substrates from the periplasm, which dissolve in the inner membrane (61, 62).

Unlike AcrA, MdtE incurred strongly negative selection at pH 5.5 in the control medium and in the presence of most tested compounds (Fig. 5A). In our gene expression assay, mdtE was upregulated in the transition to the stationary phase, a result consistent with the literature (55). This stationary-phase upregulation of MdtEF-TolC is advantageous for cells under anaerobiosis or under extreme acid exposure (11). The mdtE gene has a positive fitness contribution only when the growth cycle includes a period of extreme acid (pH 2.0) comparable to stomach passage (11). This observation is consistent with the inclusion of mdtEF in the Gad acid fitness island (slp-gadX), which is one of the most effective mechanisms of acid resistance employed by E. coli (63, 64). In our competition experiments, $mdtE^+$ showed an enhanced selection rate in the presence of salicylate or benzoate, permeant acids that acidify the cytoplasm. This could result from cytoplasmic pH depression (Fig. 3), which is part of the mechanism of acid-stress Gad induction (65).

The effects of phytochemicals on selection rates for *mdtE*⁺ and *emrA*⁺ (Fig. 5 and 6) were generally small. The relatively low expression of EmrAB-TolC suggests that deletion of the major pump AcrAB-TolC would be required to see larger effects associated with EmrAB-TolC (55). EmrAB-TolC did increase relative fitness in the presence of CCCP, although with a wide variance. Uncouplers such as CCCP and dinitrophenol are substrates and inducers for EmrAB-TolC (27, 66).

Overall, diverse selection criteria were observed among $acrA^+$, $mdtE^+$, and $emrA^+$. The effect of lipophilic non-acids on AcrAB-TolC selection appears particularly interesting. Lipophilic aromatic esters and other non-acidic molecules could offer a promising class of potential candidates for antibiotic resistance breakers. Furthermore, these molecules show clinical promise due to their minimal risk of inducing genetic resistance regulons (Table 3). Future investigation might reveal aromatic esters and other lipophilic molecules that act as resistance breakers for other pumps besides AcrAB-TolC.

MATERIALS AND METHODS

Strains and media

The experimental strains used were derived from parental strain *E. coli* K-12 W3110 (10, 48). All recombinant strains used in flow cytometry competitions contained alleles for CFP or YFP on an isopropyl β -D-1 thiogalactopyranoside (IPTG)-inducible lactose promoter (P_{L/acO-1}) (10, 11, 67) (Table 1). The strain used for cell pH depression assays contained a pH-dependent fluorophore (pHluorin) (68) on an arabinose-inducible promoter (P_{BAD}) in plasmid pGFPR01 (28). pHluorin shows excitation peaks at 410 and 470 nm that depend ratiometrically on cytoplasmic pH (68). Lab stock *E. coli* K-12 W3110 (69) was used for digital polymerase chain reaction assays.

Growth media was LBK broth (10 g/L tryptone, 5 g/L yeast extract, and 7.45 g/L potassium chloride) buffered at pH 5.5 with 100 mM 2-(N-morpholino)ethanesulfonic acid (MES; p K_a = 6.15), pH 6.8 with piperazine-N,N'-bis(2-ethanesulfonic acid) (PIPES; p K_a = 6.8), or pH 8.0 with [4-(2-hydroxyethyl)–1-piperazineethanesulfonic acid] (p K_a = 7.55). The pH was adjusted with NaOH or HCl (11). All media materials and reagents were purchased from Thermofisher unless stated otherwise: CCCP (Millipore Sigma); MES and methyl salicylate (Acros Organics); sodium ferulate (Selleck Chemicals); and salicyl alcohol (Alfa Aesar).

Minimum inhibitory concentration assays

For MIC assays with molecules used in competition experiments (see Table 2 for molecules), strains were cultured for 22–24 h in LBK pH 5.5 buffered with 0.1 M MES, with aeration, prior to MIC assay. 96-well plates were prepared by twofold serial dilution with molecules of interest. The medium used in plates was LBK 0.1 M MES pH 5.5. One microliter of overnight culture was added to each well that contained 200 μ L media (1:200). OD₆₀₀ absorbances were measured via Molecular Devices microplate reader every 15 min over 22 h (96 total reads). Plates were incubated at 37°C and shaken between reads. After 22 h, wells without growth observed were scored at or above the MIC. All antibiotic MIC assays followed the same method but used LBK pH 6.8 buffered with 0.1 M PIPES.

Flow cytometry competition assays

Flow cytometry was used to measure the relative fitness of MDR efflux pumps in short-term weekly competition experiments across ~30 generations (11, 12) (Fig. 1). All cultures were incubated at 37°C with rotation. For overnight cultures, 2 days prior to flow cytometry (Day -2), strains were cultured individually for 22–24 h in 2 mL LBK 0.1 M PIPES pH 6.8. The next day (Day -1), cultures underwent 1,000-fold dilution (2 μ L into 2 mL) into weekly competition growth media. The competition medium was LBK buffered at either pH 5.5, 6.8, or 8.0 containing a molecule of interest at 1 mM

unless stated otherwise. On Day 0, 1 mL of the pump knockout strain ($\Delta acrA::kanR$, $\Delta mdtE::kanR$, or $\Delta emrA::kanR$) was mixed (1:1) with 1 mL of the control $\Delta yhdN::kanR$ containing the opposite fluorophore. The $\Delta yhdN::kanR$ allele was included in the control strain to provide a comparable expression of kanR, which might affect relative fitness. Co-cultures then underwent 1,000-fold dilution (2 μ L into 2 mL) into fresh competition growth media prior to incubation for 22–24 h. On Days 0–2, overnight cultures were serially diluted 1,000-fold (2 μ L into 2 mL) into fresh competition growth media prior to incubation for 22–24 h.

For daily flow cytometry, overnight cocultures were diluted 100-fold (20 μ L into 2 mL) into LBK pH 6.8 0.1 M PIPES containing 1 mM IPTG to induce fluorophore expression (11, 12, 70, 71). Thus, for all cells cultured under different conditions, fluorescence was observed under a common non-selective culture condition. After 2 h incubation, cultures were diluted 20-fold into 1× phosphate-buffered saline (PBS). The cell suspensions were sampled with a BD FACSMelody Cell Sorter with a violet laser (405 nm) with a 528/45 filter for CFP, and a blue laser (488 nm) with a 545/20 filter for YFP emission. The proportions of processed events were >95%. The PBS dilution ratio was adjusted to lower the observed event rate below 10,000. Two technical replicates (each 50,000 events) were recorded, and YFP/CFP ratios were averaged. This process of recording CFP and YFP percentages was repeated for Days 0–3 of flow cytometry.

For each experimental condition tested, the selection rate for the gene tested was calculated with:

$$s = \log_2(R_t/R_0)/t$$

where R_t/R_0 represents the ratio of the control strain $\Delta yhdN$ versus the knockout strain of interest (for example, $acrA^+/\Delta acrA$) and t represents time in days with ~10 generations per day (70, 71). This calculation provides a biological indication of co-cultured genetic variants' population distribution over time. For example, a selection rate of -1 indicates that there was a twofold selection per day against the given MDR pump.

Cytoplasmic pH assays

Cytoplasmic pH was measured by flow cytometry of strain JLS1105 with the plasmid pGFPR01 expressing the ratiometric fluorophore pHluorin (28, 68). One day prior to flow cytometry, strain JLS1105 was cultured in 2 mL LBK-MES pH 5.5 and 100 μ g/mL ampicillin at 37°C with rotation for 16–20 h. Two microliters of overnight culture was diluted (1:1,000) into 2 mL of pH 5.5 0.1 M MES + 50 μ g/mL ampicillin + 0.2% L-arabinose LBK. L-arabinose was used to induce pHluorin expression from a pBAD promoter (28). The cultures were then incubated for 4.0–4.5 h.

After incubation, cultures were diluted 10-fold (100 μ L into 1 mL) with stress growth media (pH 5.5 0.1 M MES LBK with the addition of a molecule of interest). LBK pH 5.5 0.1 M MES was run at the beginning and end of all sampling sessions to ensure no significant differences over time. Five minutes after dilution, cell suspensions were sampled through BD FACSMelody. The emission intensity ratio was obtained between the 405 nm excitation (high pH) and the 488 nm excitation (low pH). A total of 50,000 events were recorded for each trial. The processed events were always more than 95%, and events rates were no more than 10,000 events/second for all samples recorded. A minimum of six biological replicates were performed for each chemical at each concentration.

Data were analyzed by converting raw fcs files to csv files using the bioconda fcsparser package. For each emission ratio, the mean, median, standard deviation, and standard error were calculated by a custom script with R and Python 3. In a given trial, if fewer than 3,000 cells were counted at 488-nm excitation, the trial was excluded from the data set to avoid noise signal from dead or non-fluorescent cells. Mean ratios were then converted to a pH value using a standard curve for pH as a function of emission ratio. The standard curve was obtained using 40 mM sodium salicylate to equilibrate cytoplasmic and external pH over the range of pH 5.5–8.0.

Digital polymerase chain reaction expression assays

One day before harvest, *E. coli* K-12 W3110 (48) were cultured in LBK 0.1 M MES pH 5.5 containing the molecule of interest for 22–24 h at 37°C with rotation for 22 h. On the day of harvest, the final optical density of *E. coli* cultures was measured with the SpectraMax Plus384 MicroPlate reader. Cultures were diluted 1,000-fold (2 μ L into 2 mL) into a fresh medium. The bacteria were cultured to the late log phase (OD₆₀₀ = 0.1–0.2) or to the transition to the stationary phase (transition phase) (OD₆₀₀ = 0.4–0.7).

For RNA extraction, 700 μL of each culture at the log phase and 500 μL of each culture at the transition phase were fixed using Bacterial RNAProtect (Qiagen, Germantown, MD, USA). RNA was extracted from the fixed culture pellets using the bacteria-specific protocols specified for the RNeasy Mini Kit (Qiagen). Following RNA extraction, RNA quality and quantity were measured with the Nanodrop One Spectrophotometer (Thermo Fisher Scientific, Waltham, MA, USA). Samples with no detectable chemical contaminants were selected for gene expression assay. Extracted RNA was stored at -80°C , as well as dilutions of 1 ng/ μ L nucleic acid for use in multiplex digital polymerase chain reaction analysis.

Probe sets for MDR pump genes *acrA*, *mdtE*, and *emrA* were designed by Integrated DNA Technologies (IDT). Each probe set was assigned a fluorescent channel in the QuantStudio Absolute Q Digital PCR System: FAM (550 nm)—*mdtE*, HEX (555 nm)—*acrA*, and TAMRA (583 nm)—*emrA*. We used $4\times$ RT Master Mix for RT-PCR reactions, $5\times$ No-RT Master Mix for no reverse transcription (no-RT) reactions (Thermo Fisher Scientific, South San Francisco, CA, USA), and ~0.9 ng of RNA for each reaction. In the dPCR system, 9 μ L of reaction mix was used for the dPCR assay, and the volume was partitioned into >20,000 nano wells. In each nano well, the distribution of templates of each assayed mRNA was assumed to follow the binomial Poisson distribution (72). The optimized dPCR protocol included the following cycling routine: 50° C/10 min; 95° C/5 s; 55° C/30 s) \times 45 cycles. For each extracted RNA sample, a no-RT PCR reaction was performed parallel to the reverse transcription reaction in dPCR to check for DNA contamination.

Statistical analysis

Mann-Whitney U tests were performed to compare flow cytometry assay selection rates to their respective pH 5.5 control (*P < 0.05, **P < 0.01, and ***P < 0.001). Welch's t-tests were performed to compare cytoplasmic pH assay results to the respective pH 5.5 control (*P < 0.05, **P < 0.01, and ***P < 0.001). Mosaic R package was used for Mann-Whitney U tests, Welch's two-sample t-tests, summary statistics, and Pearson r^2 values. Mann-Whitney U tests were used for competition assay data because they are not normally distributed. For all figures, statistical test results are presented in Table S1.

dPCR analysis was performed in R Studio. The template concentrations (copies/µL) of the three drug pump genes (*acrA*, *mdtE*, and *emrA*) were normalized to the total RNA of the sample. The template concentrations were calculated by the QuantStudio data analysis program based on a Poisson distribution (72). Two-way ANOVA and *post hoc* least squares difference with the Benjamini-Hochberg correction were used to compare expression levels of individual efflux pump genes across all tested conditions. Mosaic and Agricolae R packages were used for ANOVA and multiple comparisons.

ACKNOWLEDGMENTS

We thank Luke Smallwood for scripting the pHluorin analysis.

This work was supported by the National Science Foundation awards MCB 1923077 and MRI 1725426.

Y.L. and A.M.V.H. led the team on competition assays and drafted the full manuscript. M.T.N.P. devised the dPCR assay, led the expression analysis team, and contributed to the manuscript. B.N.N.D., R.C., S.D.R.R., K.T., D.J.F., and A.S. performed competition assays. A.P. and A.M.V.H. performed dPCR assays. A.M.V.H. and D.J.F. performed MIC assays.

C.C.M. performed competition assays and trained students. Z.C.S. mentored students and performed pHluorin and competition assays. J.L.S. conceived the study, mentored and supported students, and directed the writing of the manuscript.

AUTHOR AFFILIATION

¹Department of Biology, Kenyon College, Gambier, Ohio, USA

AUTHOR ORCIDs

Joan L. Slonczewski http://orcid.org/0000-0003-3484-1564

FUNDING

Funder	Grant(s)	Author(s)
National Science Foundation (NSF)	1923077, 1725426	Joan L. Slonczewski

AUTHOR CONTRIBUTIONS

Yangyang Liu, Conceptualization, Data curation, Formal analysis, Investigation, Methodology, Writing – original draft, Writing – review and editing | Andrew M. Van Horn, Conceptualization, Data curation, Formal analysis, Investigation, Methodology, Writing – original draft, Writing – review and editing | Minh T. N. Pham, Conceptualization, Data curation, Formal analysis, Investigation, Methodology, Writing – original draft, Writing – review and editing | Bao Ngoc N. Dinh, Data curation, Formal analysis, Investigation, Methodology, Writing – review and editing | Rachel Chen, Data curation, Investigation, Methodology | Slaybrina D. R. Raphael, Data curation, Formal analysis, Investigation, Methodology, Writing – review and editing | Alejandro Paulino, Data curation, Investigation | Kavya Thaker, Data curation, Investigation | Aaryan Somadder, Data curation, Investigation | Dominick J. Frost, Investigation | Chelsea C. Menke, Data curation, Investigation | Zachary C. Slimak, Data curation, Formal analysis, Investigation, Methodology, Project administration, Writing – original draft, Writing – review and editing | Joan L. Slonczewski, Conceptualization, Funding acquisition, Investigation, Methodology, Project administration, Supervision, Writing – review and editing

ADDITIONAL FILES

The following material is available online.

Supplemental Material

Tables S1-S3 (AEM02096-23-S0001.pdf). Supplemental tables.

REFERENCES

- Algammal A, Hetta HF, Mabrok M, Behzadi P. 2023. "Editorial: emerging multidrug-resistant bacterial pathogens "superbugs": a rising public health threat". Front Microbiol 14:1135614. https://doi.org/10.3389/ fmicb.2023.1135614
- Magiorakos AP, Srinivasan A, Carey RB, Carmeli Y, Falagas ME, Giske CG, Harbarth S, Hindler JF, Kahlmeter G, Olsson-Liljequist B, Paterson DL, Rice LB, Stelling J, Struelens MJ, Vatopoulos A, Weber JT, Monnet DL. 2012. Multidrug-resistant, extensively drug-resistant and pandrugresistant bacteria: an international expert proposal for interim standard definitions for acquired resistance. Clin Microbiol Infect 18:268–281. https://doi.org/10.1111/j.1469-0691.2011.03570.x
- Chawla M, Verma J, Gupta R, Das B. 2022. Antibiotic potentiators against multidrug-resistant bacteria: discovery, development, and clinical relevance. Front Microbiol 13:887251. https://doi.org/10.3389/fmicb. 2022.887251
- Darby EM, Trampari E, Siasat P, Gaya MS, Alav I, Webber MA, Blair JMA. 2023. Molecular mechanisms of antibiotic resistance revisited. Nat Rev Microbiol 21:280–295. https://doi.org/10.1038/s41579-022-00820-y

- Nolivos S, Cayron J, Dedieu A, Page A, Delolme F, Lesterlin C. 2019. Role of AcrAB-TolC multidrug efflux pump in drug-resistance acquisition by plasmid transfer. Science 364:778–782. https://doi.org/10.1126/science. aav6390
- Du D, Wang-Kan X, Neuberger A, van Veen HW, Pos KM, Piddock LJV, Luisi BF. 2018. Multidrug efflux pumps: structure, function and regulation. Nat Rev Microbiol 16:523–539. https://doi.org/10.1038/ s41579-018-0060-x
- Anes J, McCusker MP, Fanning S, Martins M. 2015. The ins and outs of RND efflux pumps in *Escherichia coli*. Front Microbiol 6:587. https://doi. org/10.3389/fmicb.2015.00587
- Masi M, Réfregiers M, Pos KM, Pagès JM. 2017. Mechanisms of envelope permeability and antibiotic influx and efflux in Gram-negative bacteria. Nat Microbiol 2:17001. https://doi.org/10.1038/nmicrobiol.2017.1
- Sanz-García F, Gil-Gil T, Laborda P, Blanco P, Ochoa-Sánchez LE, Baquero F, Martínez JL, Hernando-Amado S. 2023. Translating eco-evolutionary biology into therapy to tackle antibiotic resistance. Nat Rev Microbiol 21:671–685. https://doi.org/10.1038/s41579-023-00902-5

- Moore JP, Li H, Engmann ML, Bischof KM, Kunka KS, Harris ME, Tancredi AC, Ditmars FS, Basting PJ, George NS, Bhagwat AA, Slonczewski JL, Elliot MA. 2019. Inverted regulation of multidrug efflux pumps, acid resistance, and porins in benzoate-evolved *Escherichia coli* K-12. Appl Environ Microbiol 85. https://doi.org/10.1128/AEM.00966-19
- Schaffner SH, Lee AV, Pham MTN, Kassaye BB, Li H, Tallada S, Lis C, Lang M, Liu Y, Ahmed N, Galbraith LG, Moore JP, Bischof KM, Menke CC, Slonczewski JL, Kivisaar M. 2021. Extreme acid modulates fitness tradeoffs of multidrug efflux pumps MdtEF-TolC and AcrAB-TolC in *Escherichia* coli K-12. Appl Environ Microbiol 87. https://doi.org/10.1128/AEM.00724-21
- Gullberg E, Cao S, Berg OG, Ilbäck C, Sandegren L, Hughes D, Andersson DI, Lipsitch M. 2011. Selection of resistant bacteria at very low antibiotic concentrations. PLoS Pathog 7:e1002158. https://doi.org/10.1371/ journal.ppat.1002158
- Creamer KE, Ditmars FS, Basting PJ, Kunka KS, Hamdallah IN, Bush SP, Scott Z, He A, Penix SR, Gonzales AS, Eder EK, Camperchioli DW, Berndt A, Clark MW, Rouhier KA, Slonczewski JL, Elliot MA. 2017. Benzoate- and salicylate-tolerant strains of *Escherichia coli* K-12 lose antibiotic resistance during laboratory evolution. Appl Environ Microbiol 83. https: //doi.org/10.1128/AEM.02736-16
- Griffith JM, Basting PJ, Bischof KM, Wrona EP, Kunka KS, Tancredi AC, Moore JP, Hyman MRL, Slonczewski JL, Parales RE. 2019. Experimental evolution of *Escherichia coli* K-12 in the presence of proton motive force (PMF) uncoupler carbonyl cyanide m-chlorophenylhydrazone selects for mutations affecting PMF-driven drug efflux pumps. Appl Environ Microbiol 85:1–18. https://doi.org/10.1128/AEM.02792-18
- Nikaido H. 2009. Multidrug resistance in bacteria. Annu Rev Biochem 78:119–146. https://doi.org/10.1146/annurev.biochem.78.082907. 145923
- Nikaido H. 1998. Antibiotic resistance caused by Gram-negative multidrug efflux pumps. CLIN INFECT DIS 27 Suppl 1:S32–41. https://doi. org/10.1086/514920
- Thanassi DG, Cheng LW, Nikaido H. 1997. Active efflux of bile salts by *Escherichia coli*. J Bacteriol 179:2512–2518. https://doi.org/10.1128/jb. 179.8.2512-2518.1997
- Kawamura-Sato K, Shibayama K, Horii T, Iimuma Y, Arakawa Y, Ohta M. 1999. Role of multiple efflux pumps in *Escherichia coli* in Indole expulsion. FEMS Microbiol Lett 179:345–352. https://doi.org/10.1111/j. 1574-6968.1999.tb08748.x
- Li XZ, Plésiat P, Nikaido H. 2015. The challenge of efflux-mediated antibiotic resistance in gram-negative bacteria. Clin Microbiol Rev 28:337–418. https://doi.org/10.1128/CMR.00117-14
- Sayed AK, Foster JW. 2009. A 750 bp sensory integration region directs global control of the *Escherichia coli* gade acid resistance regulator. Mol Microbiol 71:1435–1450. https://doi.org/10.1111/j.1365-2958.2009. 06614.x
- Sheikh SW, Ali A, Ahsan A, Shakoor S, Shang F, Xue T. 2021. Insights into emergence of antibiotic resistance in acid-adapted enterohaemorrhagic Escherichia coli. Antibiotics (Basel) 10:522. https://doi.org/10.3390/ antibiotics10050522
- Novoa D, Conroy-Ben O. 2019. The anaerobic efflux pump MdtEF-TolC confers resistance to cationic biocides. Microbiology. https://doi.org/10. 1101/570408
- Zhang Y, Xiao M, Horiyama T, Zhang Y, Li X, Nishino K, Yan A. 2011. The multidrug efflux pump MdtEF protects against nitrosative damage during the anaerobic respiration in *Escherichia coli*. J Biol Chem 286:26576–26584. https://doi.org/10.1074/jbc.M111.243261
- Nishino K, Yamasaki S, Nakashima R, Zwama M, Hayashi-Nishino M. 2021. Function and inhibitory mechanisms of multidrug efflux pumps. Front Microbiol 12:737288. https://doi.org/10.3389/fmicb.2021.737288
- Brooun A, Tomashek JJ, Lewis K. 1999. Purification and ligand binding of EmrR, a regulator of a multidrug transporter. J Bacteriol 181:5131–5133. https://doi.org/10.1128/JB.181.16.5131-5133.1999
- Lin MF, Lin YY, Lan CY. 2017. Contribution of EmrAB efflux pumps to colistin resistance in *Acinetobacter baumannii*. J Microbiol 55:130–136. https://doi.org/10.1007/s12275-017-6408-5
- Lomovskaya O, Lewis K. 1992. Emr, an Escherichia coli locus for multidrug resistance. Proc Natl Acad Sci U S A 89:8938–8942. https://doi.org/10. 1073/pnas.89.19.8938

- Martinez KA, Kitko RD, Mershon JP, Adcox HE, Malek KA, Berkmen MB, Slonczewski JL. 2012. Cytoplasmic pH response to acid stress in individual cells of *Escherichia coli* and *Bacillus subtilis* observed by fluorescence ratio imaging microscopy. Appl Environ Microbiol 78:3706– 3714. https://doi.org/10.1128/AEM.00354-12
- Slonczewski JL, Rosen BP, Alger JR, Macnab RM. 1981. pH homeostasis in *Escherichia coli*: measurement by 31p nuclear magnetic resonance of methylphosphonate and phosphate. Proc Natl Acad Sci U S A 78:6271– 6275. https://doi.org/10.1073/pnas.78.10.6271
- Evans DF, Pye G, Bramley R, Clark AG, Dyson TJ, Hardcastle JD. 1988.
 Measurement of gastrointestinal pH profiles in normal ambulant human subjects. Gut 29:1035–1041. https://doi.org/10.1136/gut.29.8.1035
- Ibekwe VC, Fadda HM, McConnell EL, Khela MK, Evans DF, Basit AW.
 2008. Interplay between intestinal pH, transit time and feed status on the *in vivo* performance of pH responsive ileo-colonic release systems. Pharm Res 25:1828–1835. https://doi.org/10.1007/s11095-008-9580-9
- Mitchell P. 2011. Chemiosmotic coupling in oxidative and photosynthetic phosphorylation. Biochim Biophys Acta 1807:1507–1538. https://doi.org/10.1016/j.bbabio.2011.09.018
- Martins A, Spengler G, Rodrigues L, Viveiros M, Ramos J, Martins M, Couto I, Fanning S, Pagès JM, Bolla JM, Molnar J, Amaral L. 2009. pH modulation of efflux pump activity of multi-drug resistant *Escherichia* coli: protection during its passage and eventual colonization of the colon. PLoS One 4:e6656. https://doi.org/10.1371/journal.pone.0006656
- Gabel CV, Berg HC. 2003. The speed of the flagellar rotary motor of *Escherichia coli* varies linearly with protonmotive force. Proc Natl Acad Sci U S A 100:8748–8751. https://doi.org/10.1073/pnas.1533395100
- Ruiz C, Levy SB. 2014. Regulation of acrAB expression by cellular metabolites in *Escherichia coli*. J Antimicrob Chemother 69:390–399. https://doi.org/10.1093/jac/dkt352
- Abdali N, Parks JM, Haynes KM, Chaney JL, Green AT, Wolloscheck D, Walker JK, Rybenkov VV, Baudry J, Smith JC, Zgurskaya HI. 2017. Reviving antibiotics: efflux pump inhibitors that interact with AcrA, a membrane fusion protein of the AcrAB-TolC multidrug efflux pump. ACS Infect Dis 3:89–98. https://doi.org/10.1021/acsinfecdis.6b00167
- Perry EK, Meirelles LA, Newman DK. 2022. From the soil to the clinic: the impact of microbial secondary metabolites on antibiotic tolerance and resistance. Nat Rev Microbiol 20:129–142. https://doi.org/10.1038/ s41579-021-00620-w
- Divakaruni AS, Brand MD. 2011. The regulation and physiology of mitochondrial proton leak. Physiology 26:192–205. https://doi.org/10. 1152/physiol.00046.2010
- Jastroch M, Divakaruni AS, Mookerjee S, Treberg JR, Brand MD. 2010.
 Mitochondrial proton and electron leaks. Essays Biochem 47:53–67. https://doi.org/10.1042/bse0470053
- Cheng J, Nanayakkara G, Shao Y, Cueto R, Wang L, Yang WY, Tian Y, Wang H, Yang X. 2017. Mitochondrial proton leak plays a critical role in pathogenesis of cardiovascular diseases, p 359–370. In Advances in experimental medicine and biology. Springer, New York LLC.
- Brookes PS, Rolfe DFS, Brand MD. 1997. The proton permeability of Liposomes made from mitochondrial inner membrane Phospholipids: Comparison with isolated mitochondria. J Membr Biol 155:167–174. https://doi.org/10.1007/s002329900168
- Jeyakumar GE, Lawrence R. 2021. Mechanisms of bactericidal action of eugenol against *Escherichia coli*. J Herbal Medicine 26:100406. https:// doi.org/10.1016/j.hermed.2020.100406
- Waring MJ. 2009. Defining optimum lipophilicity and molecular weight ranges for drug candidates-molecular weight dependent lower log D limits based on permeability. Bioorg Med Chem Lett 19:2844–2851. https://doi.org/10.1016/j.bmcl.2009.03.109
- Aron Z, Opperman TJ. 2018. The hydrophobic trap—the achilles heel of RND efflux pumps. Res Microbiol 169:393–400. https://doi.org/10.1016/j. resmic.2017.11.001
- 45. Pos KM. 2009. Drug transport mechanism of the AcrB efflux pump. Biochim Biophys Acta 1794:782–793. https://doi.org/10.1016/j.bbapap. 2008.12.015
- 46. Cowan MM. 1999. Plant products as antimicrobial agents. Clin Microbiol Rev 12:564–582. https://doi.org/10.1128/CMR.12.4.564
- Seukep AJ, Kuete V, Nahar L, Sarker SD, Guo M. 2020. Plant-derived secondary metabolites as the main source of efflux pump inhibitors and

- methods for identification. J Pharm Anal 10:277–290. https://doi.org/10. 1016/j.jpha.2019.11.002
- 48. Hayashi K, Morooka N, Yamamoto Y, Fujita K, Isono K, Choi S, Ohtsubo E, Baba T, Wanner BL, Mori H, Horiuchi T. 2006. Highly accurate genome sequences of *Escherichia coli* K-12 strains MG1655 and W3110. Mol Syst Biol 2:2006.0007. https://doi.org/10.1038/msb4100049
- Koziolek M, Grimm M, Becker D, Iordanov V, Zou H, Shimizu J, Wanke C, Garbacz G, Weitschies W. 2015. Investigation of pH and temperature profiles in the GI tract of fasted human subjects using the intellicap® system. J Pharm Sci 104:2855–2863. https://doi.org/10.1002/jps.24274
- Wilks JC, Slonczewski JL. 2007. pH of the cytoplasm and periplasm of *Escherichia coli*: rapid measurement by green fluorescent protein fluorimetry. J Bacteriol 189:5601–5607. https://doi.org/10.1128/JB. 00615-07
- Slonczewski JL, Fujisawa M, Dopson M, Krulwich TA. 2009. Cytoplasmic pH measurement and homeostasis in bacteria and archaea, p 1–79. In Advances in microbial physiology
- Benarroch JM, Asally M. 2020. The microbiologist's guide to membrane potential dynamics. Trends Microbiol 28:304–314. https://doi.org/10. 1016/j.tim.2019.12.008
- Slonczewski JL, Macnab RM, Alger JR, Castle AM. 1982. Effects of pH and repellent tactic stimuli on protein methylation levels in *Escherichia coli*. J Bacteriol 152:384–399. https://doi.org/10.1128/jb.152.1.384-399.1982
- Salmond CV, Kroll RG, Booth IR. 1984. The effect of food preservatives on pH homeostasis in *Escherichia coli*. J Gen Microbiol 130:2845–2850. https://doi.org/10.1099/00221287-130-11-2845
- Kobayashi A, Hirakawa H, Hirata T, Nishino K, Yamaguchi A. 2006. Growth phase-dependent expression of drug exporters in *Escherichia coli* and its contribution to drug tolerance. J Bacteriol 188:5693–5703. https://doi.org/10.1128/JB.00217-06
- Mates AK, Sayed AK, Foster JW. 2007. Products of the Escherichia coli acid fitness island attenuate metabolite stress at extremely low pH and mediate a cell density-dependent acid resistance. J Bacteriol 189:2759– 2768. https://doi.org/10.1128/JB.01490-06
- Cohen SP, Levy SB, Foulds J, Rosner JL. 1993. Salicylate induction of antibiotic resistance in *Escherichia coli*: activation of the mar operon and a *mar*-independent pathway. J Bacteriol 175:7856–7862. https://doi.org/ 10.1128/jb.175.24.7856-7862.1993
- Barbosa TM, Levy SB. 2000. Differential expression of over 60 chromosomal genes in *Escherichia coli* by constitutive expression of MarA. J Bacteriol 182:3467–3474. https://doi.org/10.1128/JB.182.12.3467-3474. 2000
- Stavri M, Piddock LJV, Gibbons S. 2007. Bacterial efflux pump inhibitors from natural sources. J Antimicrob Chemother 59:1247–1260. https://doi.org/10.1093/jac/dkl460

- Waditzer M, Bucar F. 2021. Flavonoids as inhibitors of bacterial efflux pumps. Molecules 26:6904. https://doi.org/10.3390/molecules26226904
- Opperman TJ, Nguyen ST. 2015. Recent advances toward a molecular mechanism of efflux pump inhibition. Front Microbiol 6:421. https://doi. org/10.3389/fmicb.2015.00421
- Mahmood HY, Jamshidi S, Sutton JM, Rahman KM. 2016. Current advances in developing inhibitors of bacterialmultidrug efflux pumps. Curr Med Chem 23:1062–1081. https://doi.org/10.2174/-0929867323666160304150522
- Krin E, Danchin A, Soutourina O. 2010. Decrypting the H-NS-dependent regulatory cascade of acid stress resistance in *Escherichia coli*. BMC Microbiol 10:273. https://doi.org/10.1186/1471-2180-10-273
- 64. Tramonti A, De Canio M, De Biase D. 2008. GadX/GadW-dependent regulation of the *Escherichia coli* acid fitness island: transcriptional control at the *GadY-GadW* divergent promoters and identification of four novel 42 bp GadX/GadW-specific binding sites. Mol Microbiol 70:965–982. https://doi.org/10.1111/j.1365-2958.2008.06458.x
- Foster JW. 2004. Escherichia coli acid resistance: tales of an amateur acidophile. Nat Rev Microbiol 2:898–907. https://doi.org/10.1038/ nrmicro1021
- Puértolas-Balint F, Warsi O, Linkevicius M, Tang PC, Andersson DI. 2020.
 Mutations that increase expression of the EmrAB-TolC efflux pump confer increased resistance to nitroxoline in *Escherichia coli*. J Antimicrob Chemother 75:300–308. https://doi.org/10.1093/jac/dkz434
- Lutz R, Bujard H. 1997. Independent and tight regulation of transcriptional units in *Escherichia coli* via the LacR/O, the TetR/O and AraC/I1-I2 regulatory elements. Nucleic Acids Res 25:1203–1210. https://doi.org/10.1093/nar/25.6.1203
- Miesenböck G, De Angelis DA, Rothman JE. 1998. Visualizing secretion and synaptic transmission with pH-sensitive green fluorescent proteins. Nature 394:192–195. https://doi.org/10.1038/28190
- Smith MW, Neidhardt FC. 1983. Proteins induced by aerobiosis in *Escherichia coli*. J Bacteriol 154:344–350. https://doi.org/10.1128/jb.154. 1.344-350.1983
- Lenski RE, Rose MR, Simpson SC, Tadler SC. 1991. Long-term experimental evolution in *Escherichia coli*. l. adaptation and divergence during 2,000 generations. Am Nat 138:1315–1341. https://doi.org/10.1086/285289
- Dykhuizen DE. 1990. Experimental studies of natural selection in bacteria. Annu Rev Ecol Syst 21:373–398. https://doi.org/10.1146/ annurev.es.21.110190.002105
- Dube S, Qin J, Ramakrishnan R. 2008. Mathematical analysis of copy number variation in a DNA sample using digital PCR on a nanofluidic device. PLoS One 3:e2876. https://doi.org/10.1371/journal.pone. 0002876